Effect of cobalt electroless deposition on nickel hydroxide electrodes

M.G. Ortiz [a,b,*], E.B. Castro [a,1], S.G. Real [a,b,*]

[a] Instituto de Investigaciones Fisicoquímicas Teóricas y Aplicadas (INIFTA), Facultad de Ciencias Exactas, Universidad Nacional de La Plata, C.C. 16, Suc. 4, 1900 La Plata, Argentina

[b] Centro de Investigación y Desarrollo en Ciencia y Tecnología de los Materiales (CITEMA), Facultad Regional La Plata, Universidad Tecnológica Nacional, Calle 60 y 124, La Plata, Argentina

ABSTRACT

The effects of cobalt additive on the positive electrode surface of nickel alkaline batteries are investigated. Electrode surface modifications by electroless cobalt deposits were made at different immersion times. The performance of nickel hydroxide electrodes was studied by optical techniques, such as scanning electron microscopy (SEM), energy dispersive X-ray analysis (EDAX) and electrochemical methods as cyclic voltammetry, charge–discharge curves and electrochemical impedance spectroscopy (EIS). According to these results, electroless cobalt deposits obtained with 5 min of immersion time in the electroless-bath exhibit a better electrode performance.

Keywords:
Cobalt electroless
Nickel hydroxide cathodes
Alkaline batteries
Porous electrodes

Introduction

In batteries development, the current technology requires systems with higher specific energies [1–3], in which battery chemistry plays a crucial role, due to the increasing demand of portable electronic devices and electric vehicle applications. Particularly, the development and commercialization of nickel/metal hydride (Ni–MH) technology provide the possibility of producing batteries with high specific energy. The positive nickel electrode strongly influences the operation of this and others alkaline batteries. The electrochemical energy storage in the nickel hydroxide electrodes is related to the reversible insertion of H^+ into the nickel hydroxide/oxyhydroxide. Besides, reversibility of this process is an important requirement for batteries electrode materials.

It is known that low-cost pasted nickel electrode can be built on nickel foam. Nevertheless, nickel hydroxide is a p-type semiconductor and has a low conductivity; consequently an additional resistance is generated among the active material particles, the nickel substrate and the electrolyte that yields to a relatively low utilization of the active material [4,5]. To overcome this problem, battery manufacturers typically add a few percent of cobalt powder as a conductor in the lattice of nickel hydroxide. After initial oxidation, cobalt is oxidized into a highly conductive β-CoOOH [6] that ensures an efficient conductive network and leads to a higher utilization

* *Corresponding authors*. Instituto de Investigaciones Fisicoquímicas Teóricas y Aplicadas (INIFTA), Facultad de Ciencias Exactas, Universidad Nacional de La Plata, C.C. 16, Suc. 4, 1900 La Plata, Argentina. Tel.: +54 2214257430.
E-mail addresses: mortiz@inifta.unlp.edu.ar (M.G. Ortiz), sreal@inifta.unlp.edu.ar, silviareal@yahoo.com (S.G. Real).

[1] E.B. Castro passed away on February 18th, 2013.

of the nickel hydroxide. In addition, due to the irreversibility of the couple Co(III)/Co(II), β-CoOOH remains in the active material and improves their utilization and electron conductivity [7,8]. Furthermore, the incorporation of cobalt as additive in relatively large amount could result in a substantial decrease in discharge potential plateau and increase in cost [9,10]. In addition, distribution of cobalt powder on the nickel hydroxide surface can be non-uniform; hence the additive cannot effectively increase the utilization of the active material.

The electroless cobalt coating method has been previously employed as a technique for improving nickel hydroxide electrode performance [11,12]. Nevertheless, discussions about the way that electroless cobalt film affects structural and kinetic parameters are still lacking. Accordingly, in this paper we discuss the electrochemical performance of pasted nickel hydroxide electrodes after surface modifications by electroless cobalt deposits.

Experimental

Preparation of nickel hydroxide electrodes

The nickel hydroxide electrodes were prepared by mixing active material ($Ni(OH)_2$ Aldrich) and 23 wt.% PTFE, as binder material. The mixture was pasted on the nickel form substrate. The electroless surface deposition of cobalt on pasted nickel hydroxide electrodes was carried out according to experimental routines, previously described in the literature [13]: palladium (sensitization–activation process) and cobalt plating solutions. Cobalt sulfate (99.0% Mallinckrodt; 25 g l^{-1}) was used as the source of cobalt and sodium hypophosphite (99.0% Biopack; 25 g l^{-1}) as the reducing agent. The bath was stirred vigorously at 55 °C.

Three working electrodes were prepared by immersing the pasted nickel hydroxide material into the electroless cobalt plating bath at different times: 5, 15 and 30 min. They are referred in the text as electrodes:

- NiCoEL5: 5 min,
- NiCoEL15: 15 min,
- NiCoEL30: 30 min.

The corresponding geometric area and thickness are exhibited in Table 1.

Measurement procedures

The electron microscopic studies were carried out by using a scanning electron microscope Philips SEM model 505 with an image digitizer System Soft Imaging ADDA II. The EDAX mapping tests were performed using an ESEM FEI Quanta 200 model microscope. This instrument has an energy dispersive X-ray analysis system, EDAX, Apollo 40 model.

Electrochemical experiments were performed in a conventional three compartment glass cell. with 7 M KOH as electrolyte at 30 °C. A large specific area nickel mesh was employed as counter-electrode and Hg/HgO_{ss} was used as reference electrode.

The Arbin BT2000 model potentiostat was employed to perform the charge–discharge curves at different current densities and the cyclic voltammetric experiments. Full charges of the studied electrodes were obtained at $I = 0.001$ A and discharge curves, at different currents (0.00015 A–0.001 A), were registered for a cut off voltage of 0.2 V. Voltammograms were carried out at 0.005 V s^{-1} scan rate between cathodic 0.05 V and anodic 0.55 V limits respectively.

Prior to cyclic voltammetric and EIS experiments, the electrodes were activated by charge–discharge cycling until the capacity was stabilized.

EIS measurements were performed using a PAR potentiostat and a Schlumberger 1250 frequency response analyzer (19.9 mHz $\leq f \leq$ 65 kHz) and a small amplitude (0.005 V) signal perturbation to assure a constant state of discharge (SOD). EIS experiments were carried out potentiostatically at a constant SOD.

Table 1 – Geometric characteristics of working electrodes.

Electrode	Area [cm^2]	Thickness [cm]
NiCoEL5	0.38	0.12
NiCoEL15	0.40	0.11
NiCoEL30	0.40	0.11

Results and discussion

Electrode surface characterization

SEM

Fig. 1(a)–(c) exhibit the SEM micrographs, at a magnification of 8000X, of NiCoEL5, NiCoEL15, NiCoEL30 respectively. The pictures show that the surface morphologies for the NiCoEL5 and NiCoEL15 electrodes are very similar with defined holes or pores in the porous structure. However, it can be distinguish, that NiCoEL30 samples exhibit more compact morphology and closed porous structure when compared with electrodes NiCoEL5 and NiCoEL15.

EDAX

The compositional EDAX studies of the electrodes revealed the presence of Pd from the electroless solutions. This element content shows no changes, as expected, for the three studied samples since immersion time was the same (15 min) in the palladium solution. The semi quantitative EDAX elements analysis for Co, Ni and O (weight–weight percentage, wt.%) are indicated in Table 2.

These results show that Co content (wt.%) increases with immersion time in the electroless cobalt plating bath.

The cobalt distribution in the studied electrodes was analyzed by EDAX cobalt signal mapping (Figs. 2–4(b)) for the SEM areas shown in Figs. 2–4(a). These pictures indicate that cobalt signal appears to be homogenous in all the cases but its intensity increases with immersion time in the cobalt plating bath, in good agreement with Table 2 results.

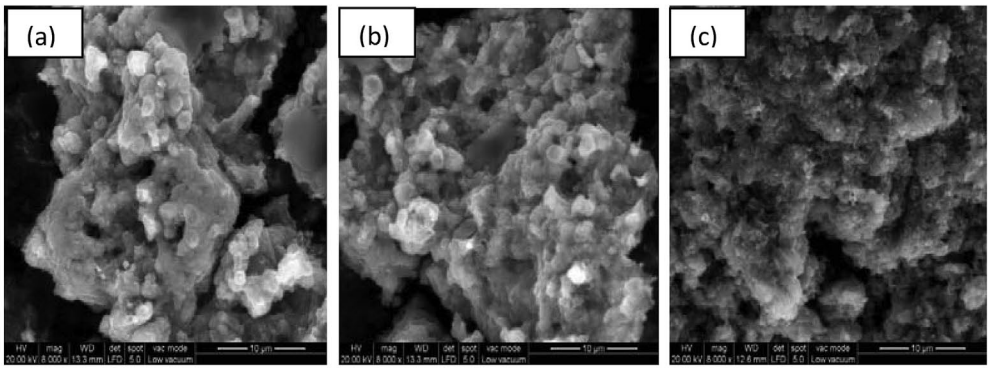

Fig. 1 – SEM micrographs (8000X): (a) NiCoEL5; (b) NiCoEL15; (c) NiCoEL30.

Table 2 – EDAX analysis of the elements.

Electrode	wt.%		
	Ni	Co	O
NiCoEL5	65.09	1.04	33.98
NiCoEL15	61.26	1.75	36.98
NiCoEL30	60.80	3.23	35.95

Electrochemical results

Voltammetric studies

Fig. 5 shows stabilized cyclic voltammetric results for each of the studied electrodes after 20 cycles. They exhibit the charge–discharge of the active material peaks associated with oxidation–reduction $Ni(OH)_2/NiOOH$ pair.

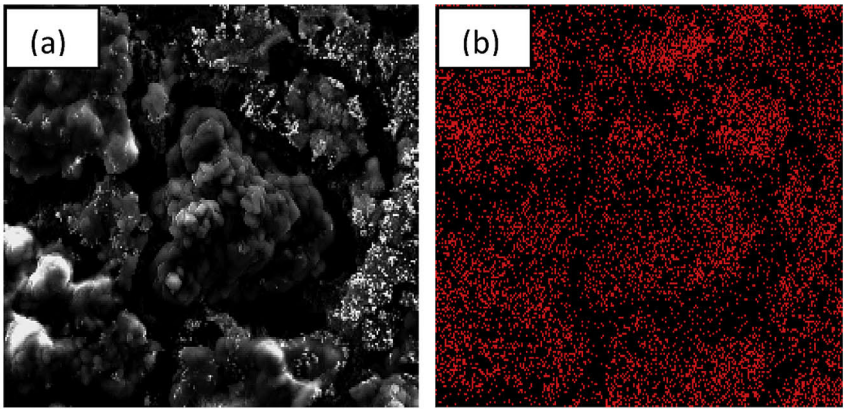

Fig. 2 – NiCoEL5 electrode (a) SEM at 5000X; (b) EDAX Co distribution.

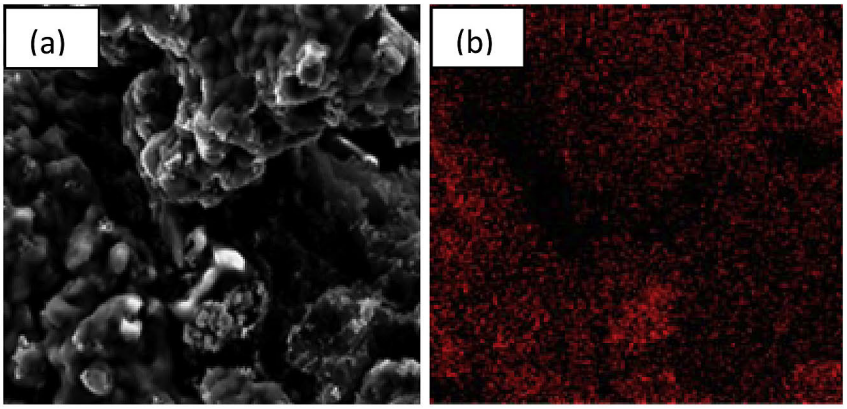

Fig. 3 – NiCoEL15 electrode: (a) SEM at 5000X; (b) EDAX Co distribution.

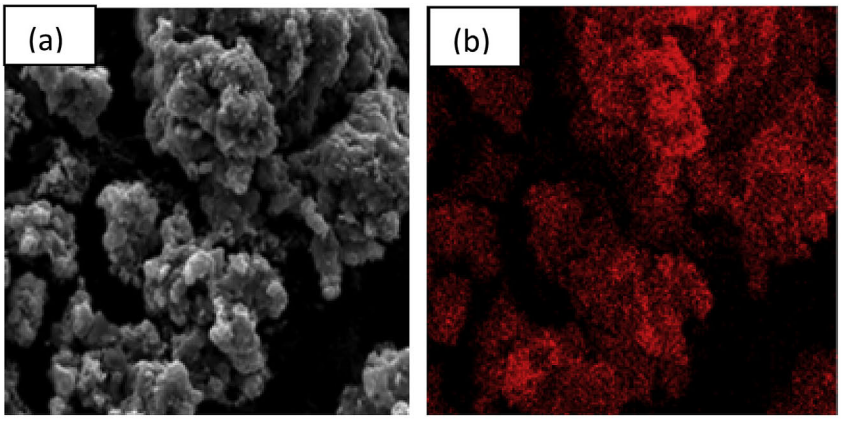

Fig. 4 – NiCoEL30 electrode: (a) SEM at 5000X; (b) EDAX Co distribution.

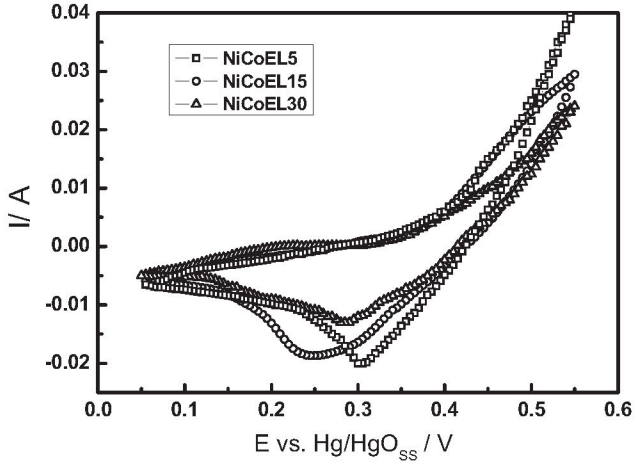

Fig. 5 – Cyclic voltammetry results for the studied electrodes after 20 cycles at 0.05 V s^{-1}.

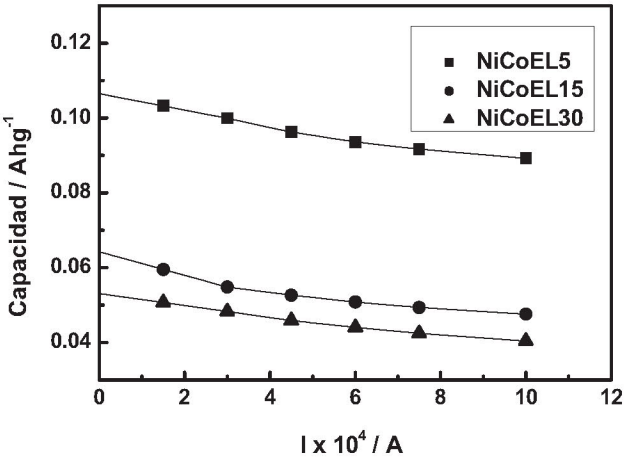

Fig. 6 – Capacity at different discharge currents.

In spite of anodic potential peak values (Epa) are not very well defined for electrodes NiCoEL15 and NiCoEL30, due to the overlapping of oxygen evolution reaction with the $Ni(OH)_2$/NiOOH process, it is apparent that these values are similar for all the studied electrodes. However, Fig. 5 clearly shows that cathodic potential peak value (Epc) for electrode NiCoEL5 is more positive. Consequently, we can conclude that the voltammetric response of electrode NiCoEL5 shows a better reversibility of these process (< <DELTA>Epa,pc).

Galvanostatic discharge curves

Fig. 6 displays the electrode capacity response for the three studied samples, at different discharge currents (from low to high currents). Before each discharge curve the electrode underwent a full charge to full capacity. It can be seen that the graphs exhibit similar slopes but different intercepts. Each electrode has a maximum discharge capacity, whose values are obtained from extrapolation to $I = 0$ in Fig. 6 and are presented in Table 3. It can be seen that electrode NiCoEL5 shows a higher maximum discharge capacity value than their corresponding to NiCoEL15 and NiCoEL30 electrodes. This maximum discharge capacity value obtained for electrode NiCoEL5 (0.108 Ah g^{-1}) is still far from that corresponding to the theoretical value (0.289 Ah g^{-1}) [14] and also is 50% lower that some reported commercial values [15,16]. These facts clearly indicate that further efforts and investigations are required in this direction.

Cycling life investigations

The evaluation of cycling life was carried out by applying consecutive charge–discharge cycles. Fig. 7 exhibits, for each electrode, the evolution of capacity vs. discharge cycles at

Table 3 – Maximum discharge capacity values.

Electrode	Maximum capacity [Ah g^{-1}]
NiCoEL5	0.108
NiCoEL15	0.064
NiCoEL30	0.052

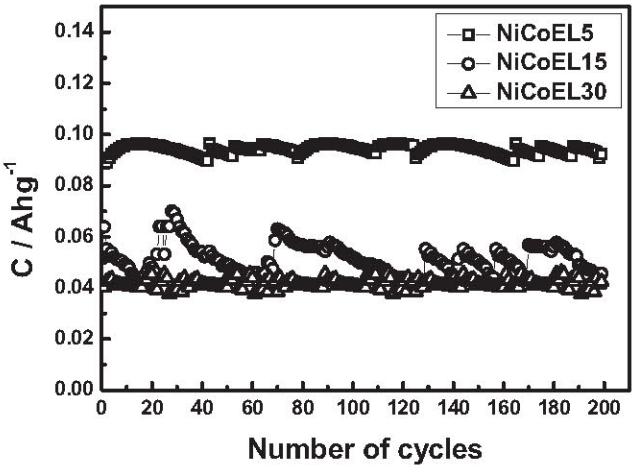

Fig. 7 – Discharge capacity vs. number of cycling.

0.75 C, C being the maximum capacity. The graph shows discharge capacity values during cycling with the smallest average value for NiCoEL30 electrode and the highest one for NiCoEL5 (0.092 Ah g^{-1} averaged value). In spite of capacity changes with cycling were evident for electrode NiCoEL15, very small changes were exhibited for electrodes NiCoEL5 and NiCoEL30.

Experimental EIS data and fitting results

Fig. 8(a)–(c) display the Nyquist plots, at a fixed SOD of 20%, for electrodes NiCoEL5, NiCoEL15 and NiCoEL30 respectively. These impedance diagrams show similar general features. In the high frequency range a linear behavior with a slope of approximately 45° is exhibited, a typical response related to a porous structure. At intermediate frequencies, a charge transfer resistance process is observed. Furthermore, in the low frequency interval, the diffusion impedance is defined.

Experimental EIS data are fitted to the theoretical impedance function (Zp), derived from the previously reported model, using the Nelder-Meade simplex search algorithm included in the Matlab package [9,17–22]. The physicochemical model describes the working electrodes as a porous structure, flooded with a highly concentrated electrolyte (KOH 7 M) and with the charge/discharge processes occurring at the active material/electrolyte interface. The nickel electrode is assumed as conformed by spherical NiOOH particles deposited on a conducting support.

The comparison of the theoretical Z_P function with the experimental impedance spectra, allows the kinetic and structural parameters of the system to be identified, such as: double layer capacitance per unit volume (C_{DC} [F cm^{-3}]), interfacial area per unit volume (a_e [cm^2 cm^{-3}]), effective conductivity (k [Ω cm^{-1}]), diffusion coefficient (D [cm^2 s^{-1}]), exchange current density (i_0 [A cm^{-2}]) [21].

The EIS fitted results exhibit a fairly good agreement between theoretical and experimental data (Figs. 9–11).

According to the fitting procedure, the characteristic parameter values are presented in Table 4. They showed a fairly good reproducibility, within 10% of experimental error.

Table 4 exhibits that, for a constant SOD and increasing time in the electroless bath, C_{DC}, a_e and k values diminish. These features can be understood taking into consideration that for increasing time in the electroless bath, the deposition of cobalt in the porous surface of the active material is increased. These facts would be responsible of building blocking regions which disconnect the active material structures that no longer participate in the electrochemical processes.

The estimated diffusion coefficient values, presented in Table 4, are in good agreement with those reported in the literature [23,24].

The exchange current density value i_0 (Table 4) estimated for electrode NiCoEL5 it appears to be higher than those for NiCoEL15 and NiCoEL30.

Taking into account these results we can conclude that the better electrochemical performance of electrodes NiCoEL5 (higher capacity values and improved reversibility) can be mainly associated with to their higher structural (a_e and k) and kinetic parameters values (i_0).

All these facts can be understood considering that shorted electroless immersion time (5 min) allow improving the distribution of cobalt deposits on the porous structure of nickel hydroxide surface. However, for 15 and 30 min immersion in electroless bath, it is apparent from EDAX and impedance results (higher Co intensity and lower structural parameters values a_e and k) that blocking regions in the porous nickel hydroxide structure would disconnect the active material sites.

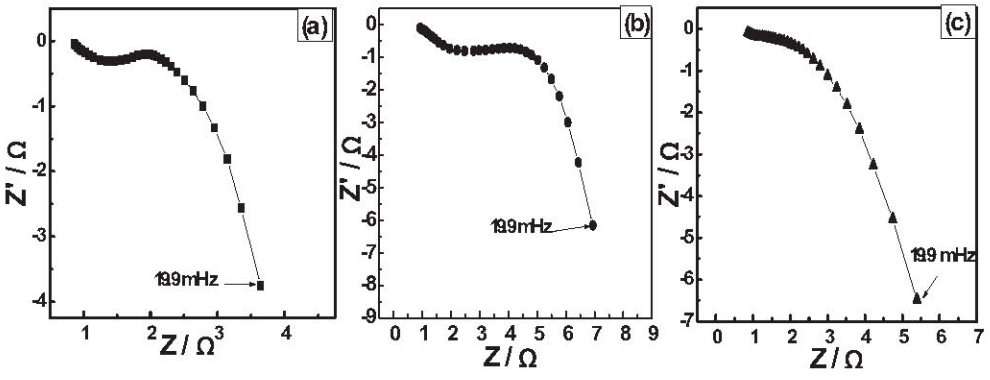

Fig. 8 – Nyquist plots, at SOD of 20%, for electrodes: (a) NiCoEL5; (b) NiCoEL15 and (c) NiCoEL30.

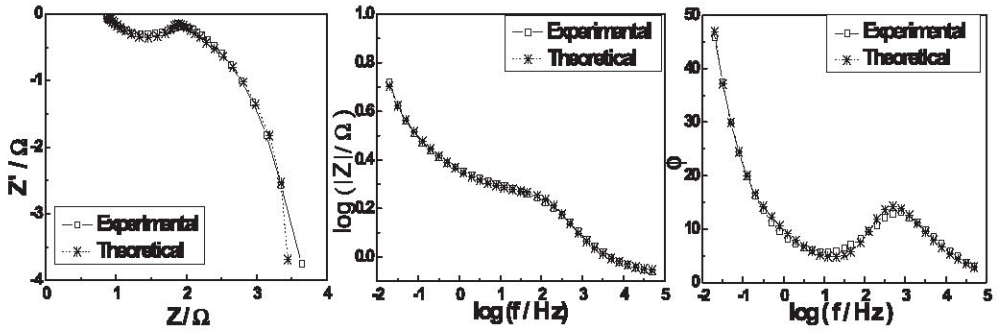

Fig. 9 – Theoretical and experimental impedance diagrams, at SOD of 20%, for electrode NiCoEL5.

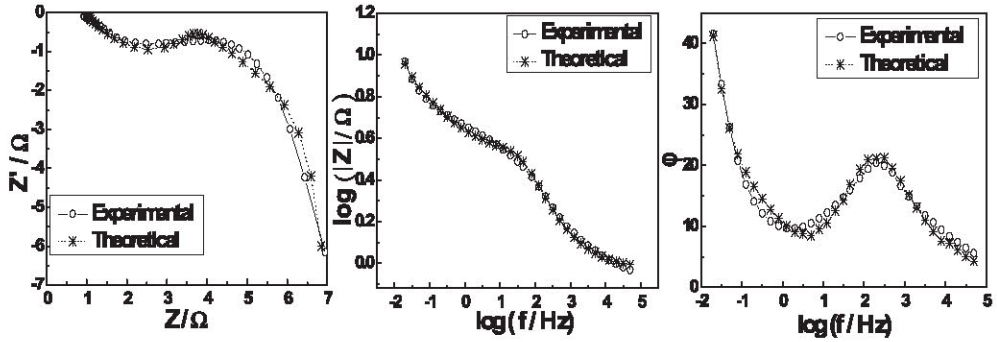

Fig. 10 – Theoretical and experimental impedance diagrams, at SOD of 20%, for electrode NiCoEL15.

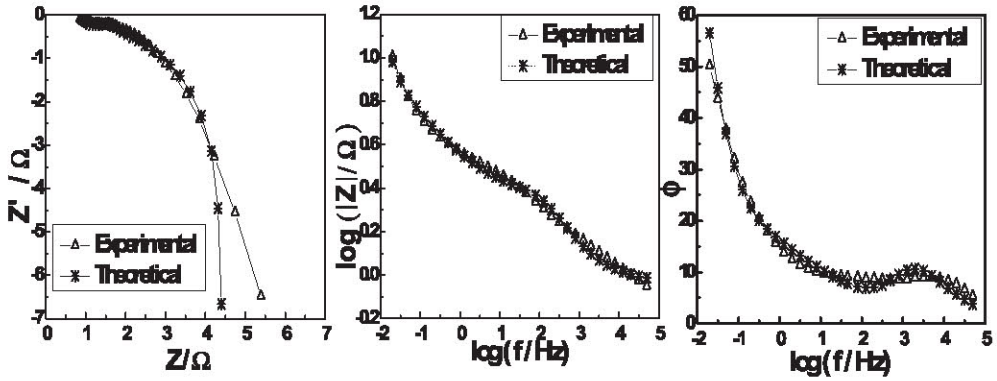

Fig. 11 – Theoretical and experimental impedance diagrams, at SOD of 20%, for electrode NiCoEL30.

A possible explanation of the observed results is based on obtaining a well spread cobalt film containing highly conductive β-CoOOH species in the porous nickel electrode. This coating would cause good electrical connection of the whole porous active structures (nickel hydroxide particles and nickel substrate) that would participate in the electrochemical processes. Furthermore, the cobalt additive effectively increases the utilization of the nickel active material since allows the nickel to reach a higher oxidation state after charging [8].

Table 4 – Characteristic parameters obtained from the fitting procedure.

Electrode	SOD	C_{DC} [F cm^{-3}]	k [Ω^{-1} cm^{-1}]	a_e [cm^{-1}]	D [cm^2 s^{-1}]	i_0 [A cm^{-2}]
NiCoEL5	20	0.135	0.047	2700	8.3×10^{13}	1.5×10^{3}
NiCoEL15	20	0.110	0.040	2200	8.3×10^{13}	4.0×10^{4}
NiCoEL30	20	0.089	0.023	1786	1.0×10^{13}	8.5×10^{4}

Conclusions

From capacity results, we can conclude that cobalt deposits obtained with 5 min of immersion in the electroless bath (NiCoEL5) allow improving electrochemical behavior of the $Ni(OH)_2$ active material (around 107% more than that corresponding to NiCoEL30). Taking into consideration the fitting procedure and the identification of characteristic parameters exhibit in Table 4, it is apparent that NiCoEL5 type's electrodes exhibit higher active area per unit volume (a_e), effective conductivity (k) and exchange current density (i_0) values. These facts are mainly responsible of the increase in the discharge capacity values and the better reversibility of the peaks associated with oxidation–reduction pair.

Acknowledgments

The financial support given by the following Argentina organizations: Agencia Nacional de Promoción Científica y Tecnológica (ANPCyT), Consejo Nacional de Investigaciones Científicas y Técnicas (CONICET) and Universidad Tecnológica Nacional (UTN) is gratefully acknowledged by the authors.

REFERENCES

[1] Dhar SK, Ovshinsky SR, Gifford PR, Corrigan DA, Fetcenko MA, Venkatesan S. Nickel/metal hydride technology for consumer and electric vehicle batteries – a review and up-date. J Power Sources 1997;65(1–2):1–7.

[2] Coates DK, Fox CL, Miller LE. Hydrogen-based rechargeable battery systems: military, aerospace, and terrestrial applications – I. Nickel–hydrogen batteries. Int J Hydrogen Energy 1994;19(9):743–50.

[3] Feng F, Geng M, Northwood DO. Electrochemical behavior of intermetallic-based metal hydrides used in Ni–metal hydride (MH) batteries: a review. Int J Hydrogen Energy 2001;26:725–34.

[4] Zimerman AH, Effa PK. Discharge kinetics of the nickel electrode. J Electrochem Soc 1984;131:709–13.

[5] Barand R, Randell CF, Tye FL. Studies concerning charged nickel hydroxide electrodes I. Measurement of reversible potentials. J Appl Electrochem 1980;39:109.

[6] Pralong V, Delahaye-Vidal A, Beaudoin B, Leriche J-B, Tarascon J-M. Electrochemical behavior of cobalt hydroxide used as additive in the nickel hydroxide electrode. J Electrochem Soc 2000;147(4):1306–13.

[7] Armstrong RD, Briggs GW, Charles EA. Some effects on the addition of cobalt to the nickel hydroxide electrode. J Appl Electrochem 1988;18:215–9.

[8] Li Xiaofeng, Dong Huichao, Zhang Hualin. An improvement on redox reversibility of cobalt oxyhydroxide in nickel hydroxide electrodes. Mater Chem Phys 2008;111:331–4.

[9] Ortiz MG, Castro EB, Real SG. The cobalt content effect on the electrochemical behavior of nickel hydroxide electrodes. Int J Hydrogen Energy 2012;37:10365–70.

[10] Ken-ichi Watanabe, Mitsuru Koseki, Naoaki Kumagai. Effect of cobalt addition to nickel hydroxide as a positive material for rechargeable alkaline batteries. J Power Sources 1996;58:23–8.

[11] Wang X, Yan J, Yuan H, Zhou Z, Song D, Zhang Y, et al. Surface modification and electrochemical studies of spherical nickel hydroxide. J Power Sources 1998;72:221.

[12] Wang Xianyou, Luo Hean, Yang Hongping, Sebastian PJ, Gamboa SA. Oxygen catalytic evolution reaction on nickel hydroxide electrode modified by electroless cobalt coating. Int J Hydrogen Energy 2004;29:967–72.

[13] Huang XH, Yuan YF, Wang Z, Zhang SY, Zhou F. Electrochemical properties of NiO/Co–P nanocomposite as anode materials for lithium ion batteries. J Alloys Compd 2011;509:3425–9.

[14] Nathira Begum S, Muralidharan VS, Ahmed Basha C. The influences of some additives on electrochemical behaviour of nickel electrodes. Int J Hydrogen Energy 2009;34:1548–55.

[15] Gifford Paul, Adams John, Corrigan Dennis, Venkatesan Srinivasan. Development of advanced nickel metal hydride batteries for electric and hybrid vehicles. J Power Sources 1999;80:157–63.

[16] Chen Dong, Cheng Jie, Wen Yuehua, Pan Junqing, Cao Gaoping, Yang Yusheng. Study of nickel-plated monolithic porous carbon as a substrate for nickel hydroxide electrode. Int J Electrochem Sci 2013;8:6467–77.

[17] De Levie R. In: Delahay P, editor. Advances in electrochemistry ad electrochemistry engineering, 6. NY: Interscience; 1967. pp. 329–61.

[18] Meyers JP, Doyle M, Darling RM, Newman J. The impedance response of a porous electrode composed of intercalation particles. J Electrochem Soc 2000;147:2930–40.

[19] Motupally S, Streinz CC, Weidner JW. Proton diffusion in nickel-hydroxide films: measurement of the diffusion coefficient as a function of state of charge. J Electrochem Soc 1995;142:1401–8.

[20] Castro EB, Cuscueta DJ, Milocco RH, Ghilarducci AA, Salva HR. An EIS based study of a Ni–MH battery prototype. Modeling and identification analysis. Int J Hydrogen Energy 2010;35:5991.

[21] Real SG, Ortiz MG, Castro EB, Visintin A, Becker D, Garaventta G. Dynamic monitoring of structural changes in nickel hydroxide electrodes during discharge in batteries. Electrochim Acta 2011;56(23):7946–54.

[22] Jacobsen T, West K. Diffusion impedance in planar, cylindrical and spherical symmetry. Electrochim Acta 1995;40:255.

[23] Zhang Chaojiong, Park Su-Moon. The anodic oxidation of nickel in alkaline media studied by spectroelectrochemical techniques. J Electrochem Soc 1987;134(12):2966–70.

[24] Mao Z, De Vidts P, White RE, Newman J. Theoretical analysis of the discharge performance of a $NiOOH/H_2$ cell. J Electrochem Soc 1994;141:54–64.